Eur. Phys. J. D **12**, 133–146 (2000)

**THE EUROPEAN PHYSICAL JOURNAL D**

EDP Sciences


# Theoretical study of energy transfer in Rb(7S) + Rb(5S) and Rb(5D) + Rb(5S) collisions

K. Orlovsky[1,a], V. Grushevsky[1], and A. Ekers[2,b]

[1] University of Latvia, Institute of Atomic Physics and Spectroscopy, Raina bulv. 19, 1586 Riga, Latvia
[2] University of Kaiserslautern, Dept. of Physics, Postfach 3049, 67653 Kaiserslautern, Germany

Received 13 November 1998 and Received in final form 22 November 1999

**Abstract.** We present results of theoretical studies of the non-resonant excitation transfer in Rb(7S) + Rb(5S) and Rb(5D) + Rb(5S) collisions at thermal collision energies. $Rb_2$ adiabatic molecular terms correlating with the 5S+7S, 5S+5D and 5P+5P states of separated atoms were calculated for internuclear distances $R > 20$ a.u. using asymptotic approximation. Mechanisms of collisional population and quenching of the 5D state were treated on the basis of the computed molecular terms, and the respective cross-sections were calculated. Theoretical cross-sections are in good agreement with the experimental values at thermal collision energies ($T \sim 500$ K).

**PACS.** 34.50.Fa Electronic excitation and ionization of atoms (including beam-foil excitation and ionization) – 34.20.-b Interatomic and intermolecular potentials and forces, potential energy surfaces for collisions

## 1 Introduction

Excitation energy transfer (ET) in atomic collisions is a subject of intense studies over several decades. Until the middle of 70-ties, mainly ET between the resonance states in alkalis was studied (see review [1] and references therein). To interpret these processes theoretically, the theory of non-adiabatic processes had been developed ([2] and references therein). In 70-ties, ET was observed in a collisions of two excited alkali atoms in resonance states leading to formation of one highly excited atom and one atom in ground state (the so-called energy pooling (EP)) [3,4]:

$$\mathrm{A}^*(n_1\mathrm{P}_{j_1}) + \mathrm{B}^*(n_2\mathrm{P}_{j_2}) \rightarrow \mathrm{A}^{**}(n_3 l_{j_3}) + \mathrm{B}(n_0\mathrm{S}_{1/2}) + \Delta E.$$

Already the first theoretical studies of EP showed that its high efficiency is related with the strong dipole-dipole interaction between the initial and final states [5–7]. The EP has been studied since then in both homonuclear [8–13] and heteronuclear [14–16] collisions, and elaborated experiments have been performed with polarised collision partners [17]. The theoretical calculations of ET show that the results depend on factors like the chosen basis set of molecular wave functions, included interactions, quality of the molecular terms used in calculations, and the approach used for calculations of the dynamics of collision process. One can notice that calculations tend to give cross-sections systematically lower than the experimental values (see [6] and compare [9,10] with [7,18,19]). The difficulties persist also in interpretation [18,20] of the polarisation dependent experimental data [20] for the EP of two Na(3P) atoms. Note, that for several experimental studies either no theoretical counterparts exist [11,12,14,15], or they are incomplete [13,16].

Recently a rather large cross-section $\sigma(500\ \mathrm{K}) = (8 \pm 4) \times 10^{-15}$ cm$^2$ had been measured for the ET process [21]

$$\mathrm{Rb(7S)+Rb(5S)} \rightarrow \mathrm{Rb(5D)+Rb(5S)} + \Delta E = 607\ \mathrm{cm}^{-1}, \quad (1)$$

where initial and final atomic states seemingly do not possess the dipole coupling. The 5D state collisional quenching cross-section $\sigma_q^{5\mathrm{D,exp}} = (2 \pm 1) \times 10^{-14}$ cm$^2$ was also reported in the same work. Despite the "dipole-forbidden" appearance of the process (1), this kind of reactions were observed to proceed efficiently also in other alkalis [22]. In our earlier theoretical study [23] we have shown that the observed efficient ET between the 7S and 5D states of Rb is thanks to the near lying 5P+5P configuration, which introduces a strong dipole coupling between the initial 7S+5S and final 5D+5S configurations. In the present work we give a more detailed description of the method, and generalise the calculations for both exo- and endoenergetic processes.

In general, inelastic collisions of type $\mathrm{A} + \mathrm{B}^* \rightarrow \mathrm{A}^* + \mathrm{B} \pm \Delta E$ at thermal collision energies can be considered as transitions between quasi-molecular terms corresponding to initial and final states of a system of colliding atoms.

[a] e-mail: korlovsk@latnet.lv
[b] e-mail: ekers@physik.uni-kl.de

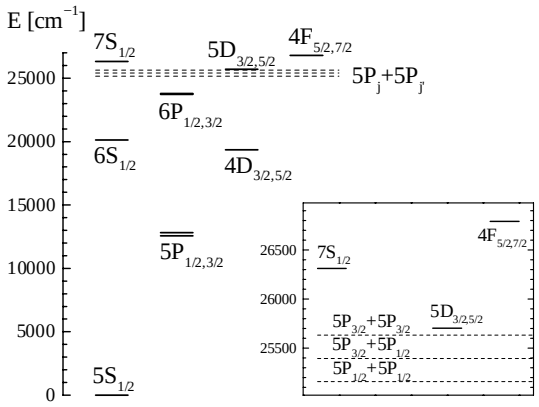


**Fig. 1.** The lowest energy levels of Rb atom. Broken lines represent energies of the $5P_j + 5P_{j'}$ states.

Such processes take place at localised regions around internuclear distances where molecular terms exhibit crossings or avoided crossings. If the electronic states of $A+B^*$ and $A^*+B$ are connected with optical dipole transitions, inelastic processes may proceed efficiently at large internuclear distances thanks to dipole-dipole interaction. Theoretical treatment of ET requires information on the interatomic interactions at medium and large internuclear distances ($R \geq 20$ a.u.). Essential is the qualitative picture of terms, which allows one to determine locations and parameters of term crossings and avoided crossings. For the excited $Rb_2$ states of interest, the potential curves have never been calculated quantum mechanically for a broad range of internuclear distances. To calculate the adiabatic molecular terms, we use a comparatively simple asymptotic method [24]. Since the positioning of electronic terms correlating with 5P+5P, 5D+5S and 7S+5S is such that they are well separated from the other higher and lower lying states (see Fig. 1), the processes of ET between the 7S and 5D states and their quenching can be treated as non-adiabatic transitions within this particular group of terms.

In this study we have improved the terms given in [23]. This specification has influenced the layout of terms shifting and the absolute positioning of crossings and avoided crossings. The transition probabilities between the atomic sates remained practically unchanged, but the effective cross-section for the reaction (1) somewhat increased, which is an effect of shift of the non-adiabatic regions towards larger internuclear distances. The fact that the dependence of the cross-section on the absolute values of term energies and parameters of most of the avoided crossings is weak supports the conclusion drawn in [23] that the considered processes are close to statistical. Relying on the calculated terms, we were able to determine the partial populations of the molecular states and the corresponding populations of atomic states at infinite internuclear separation at a unity initial population of a selected molecular state. This allowed us to calculate transition probabilities for a large number of collisional processes.

## 2 Interatomic interactions and molecular terms at large internuclear distances

Relatively large experimental cross-sections for the process (1) and 5D quenching suggest that the main contribution to these processes is due to non-adiabatic transitions at large internuclear distances, $R > 20$ a.u., for which a system of adiabatic electronic terms should be built correlating with the initial and final states of separated atoms, 7S+5S, 5D+5S, and 5P+5P (hereafter – SS, DS, and PP, respectively). Adiabatic electronic terms for these highly excited $Rb_2$ states are not known, and exact calculation of them is an extremely complicated computational task. To avoid this problem, we have used a simple and well-approved asymptotic method [24]. Comparison of quantum mechanical and asymptotic calculations has shown [25] that the asymptotic method gives a correct relative disposition and slope of molecular terms at internuclear distances $R \geq 2(1/\alpha_B - 1/\alpha_A)$, and provides in most cases also satisfactory estimates of their absolute energies. Here $\alpha_{A,B} = \sqrt{2I_{A,B(SL)}}$, where $I_{A,B(SL)}$ is the first ionisation potential of a ground state (A) or excited (B) atom in SL state.

### 2.1 Hamiltonian

In a rotating system of molecular coordinates, the Hamiltonian of a colliding pare can be written as

$$\hat{H} = \hat{H}_A + \hat{H}_B + \hat{V} + \hat{V}_R + \omega\hat{j}_\perp + \hat{V}_{SO}, \qquad (2)$$

where $\hat{H}_A$ and $\hat{H}_B$ are the Hamiltonians of isolated atoms; $\hat{V}$ is the interaction operator between atoms A and B; $\hat{V}_R$ and $\omega\hat{j}_\perp$ are the operators of radial coupling and Coriolis interaction respectively, $\hat{V}_{SO}$ denotes the operator of spin-orbit interaction, which is practically independent of the internuclear distance for $R \gg 15$ and equals the sum of the corresponding operators in atoms.

At large internuclear distances interaction of atoms weakens and becomes comparable with the spin-orbit splitting (237.6 cm$^{-1}$) of the rubidium $5P_{1/2,3/2}$ doublet. Therefore it is convenient to use adiabatic $\Omega$ basis, in which the spin-axis interaction is accounted for in molecular wave functions. In this case, besides the projection of total electronic angular moments onto internuclear axis, $\Omega$, the adiabatic terms are characterised also by parity ($w = +1, -1$ for $g, u$) of the wave function regarding inversion $\hat{W}$ in the centre of the molecule and, for terms with $\Omega = 0$, also by symmetry ($\sigma = +, -$) of the reflection $\hat{\sigma}_V$ through a plane containing internuclear axis. The action of the symmetry operators on the basis functions is given in [5].

As the basis of zero order approximation we chose eigenfunctions of the Hamiltonian of separated atoms

$$\hat{H}_0 = \hat{H}_A + \hat{H}_B + \hat{V}_{SOA} + \hat{V}_{SOB}, \qquad (3)$$

where $\hat{V}_{SOA}$, $\hat{V}_{SOB}$ are the spin-orbit interaction operators in atoms A and B. At large internuclear distances

the molecular wave functions $|\Omega_w^\sigma\rangle$ can be constructed by means of the projection operator technique as linear combinations of antisymmetrised multiplications of wave functions of isolated atoms $\langle j_1^{\rm A} m_1 | \langle j_2^{\rm B} m_2 |$. One accounts here only for the atomic states correlating with a given molecular state. In order to build molecular terms in this approximation, it is necessary to diagonalise the matrix with matrix elements of the form [5]

$$H_{if} = {}_i\langle j_1^{\rm A} m_1 |_i \langle j_2^{\rm B} m_2 | \hat{H}(1 - \hat{A} + w\hat{W} + \sigma\hat{\sigma}_V - w\hat{A}\hat{W} + \sigma w\hat{W}\hat{\sigma}_V - \sigma\hat{A}\hat{\sigma}_V - \sigma w\hat{A}\hat{W}\hat{\sigma}_V) \times |j_1'^{\rm A} m_1'\rangle_f |j_1'^{\rm B} m_2'\rangle_f, \quad (4)$$

where $\hat{H}$ is the Hamiltonian (2) of the molecule without the operators of non-adiabatic couplings $\hat{V}_{\rm R}$ and $\omega\hat{j}_\perp$ and the operator of spin-orbit interaction, $\hat{A}$ is the antisymmetrisator, $j_1^{\rm A}$ , $j_2^{\rm B}$ are the total moments of isolated atoms A and B, and $m_1, m_2$ are their projections onto internuclear axis; $|m_1 + m_2|_i = |m_1' + m_2'|_f = \Omega$.

Since the overlap of atomic wave functions at large internuclear distances is small, the parts containing squares of overlap integrals can be disregarded. Moreover, if one assumes that distortion of the wave functions, which has to be taken into consideration in correct asymptotic calculations of exchange interaction, is small and has no influence on the magnitude of Coulomb interaction, the operator of interatomic interaction $\hat{V}$ becomes [26]

$$\hat{V} = \hat{V}_{\rm Coul} + \hat{V}_{\rm disp} + \hat{V}_{\rm exch}, \quad (5)$$

with $\hat{V}_{\rm Coul}$ being the operator of Coulomb interaction, which can be factorised to multipoles, $\hat{V}_{\rm disp}$ – the effective operator of dispersion interaction, and $\hat{V}_{\rm exch}$ – the operator of exchange interaction of electrons $1_{\rm A}$ and $2_{\rm B}$ between each other and with another nucleus. We used the atomic wave functions, the radial parts of which at large internuclear distances were expressed as

$$\varphi_{nl}(R) = N_{nl} R^{1/\alpha_{nl}-1} {\rm e}^{-\alpha_{nl}R}, \quad (6)$$

where $\alpha_{nl}^2/2$ is the binding energy of $nl$ valence electron. The normalising coefficient $N_{nl}$ can be calculated either in Coulomb's approximation, which provides satisfactory accuracy for excited states of alkalis, or by matching expression (6) with Hartree-Fock calculations of the wave function at the atomic size limit. Using the function (6), the matrix elements (4) are readily calculable by methods of the theory of atomic spectra [27]. The values of the asymptotic parameters used in the calculations are given in Table 1.

**Table 1.** Asymptotic parameters of valence electron in atom or in negative ion.

| Atom or negative ion | $nl$-state of the valence electron | $N_{nl}$ or $N_i$ (a.u.) | $\alpha_{nl}$ or $\beta$ (a.u.) |
|---|---|---|---|
| Rb($5^2S_{1/2}$) | 5s | 0.49* | 0.554 |
| Rb($7^2S_{1/2}$) | 7s | 0.002** | 0.259 |
| Rb($5^2P_{1/2}$) | 5p | 0.116** | 0.4386 |
| Rb($5^2P_{3/2}$) | 5p | 0.113** | 0.436 |
| Rb($5^2D_{3/2}$) | 5d | 0.0014** | 0.270 |
| Rb($5^2D_{5/2}$) | 5d | 0.0014** | 0.270 |
| $Rb^-(^1S_0)$ | 5s | 1.5*** | 0.189 |

* Matching with Hartree-Fock wave function.
** Calculated for electron in Coulomb field of the core ion [24].
*** Reference [39].

## 2.2 Diagonal interactions

Let us consider the main interactions in the $Rb_2$ system at large internuclear distances. At distances larger than 45 a.u. the atoms in all configurations can be regarded as free. At $20 \le R \le 45$ a.u. the exchange interaction dominates within the SS and DS configurations. In the basis of $|\Omega_w^\sigma\rangle$ the matrix elements of $\hat{V}_{\rm exch}$ are diagonal and contain all possible two-electron exchange integrals. These integrals can be expressed through asymptotic splitting of singlet and triplet states, which occur at the interaction of two hypothetical single-electron atoms with the electronic wave functions corresponding to atomic orbitals of type (6). The exchange integrals were calculated by means of asymptotic formulae given in [28]. Among the large number of exchange integrals in the SS and DS configurations, the main contribution to the matrix elements (4) is due to the exchange integrals without excitation transfer with zero projection of electronic orbital moments onto internuclear axis, the $Y_\Sigma$ integrals. The other integrals did not exceed a few per cent of $Y_\Sigma$, and were therefore treated as small corrections.

Within the PP configuration there exists a direct electrostatic interaction proportional to $1/R^5$, which corresponds to interaction of atomic quadrupole moments. However, the quadrupole interaction does not exceed 30 $\rm cm^{-1}$ and can be therefore disregarded for the considered range of internuclear distances.

The dispersion interaction has a form $-C/R^6$ for all configurations. To estimate the dispersion interaction we used the formulae given in [25,28]:

*see equations (7, 8) below.*

$$\langle\langle j_1^{\rm A} m_1 S_1 0 | \langle j_2^{\rm B} m_2 (nl)^{N_2} S_2 L_2 \| \hat{V}_{\rm disp} \| j_1^{\rm A} m_1 S_1 0\rangle | j_2'^{\rm B} m_2 (nl)^{N_2} S_2 L_2'\rangle\rangle = \frac{\alpha_{\rm A}\langle r_{\rm B}^2\rangle_{nl}}{R^6}\sqrt{\frac{6}{5}}\sqrt{2j_2+1}(-1)^{L_2+S_2+j_2} \times \begin{bmatrix} j_2' & 2 & j_2 \\ m_2 & 0 & m_2 \end{bmatrix} \begin{Bmatrix} L_2 & j_2 & S_2 \\ j_2' & L_2' & 2 \end{Bmatrix} \langle (nl)^{N_2} S_2 L_2 \| U^2 \| (nl)^{N_2} S_2 L_2'\rangle, \quad (7)$$

$$\langle r_{\rm B}^2\rangle_{nl} = \int_0^\infty r^2 \varphi_{nl}^2(r) r^2 {\rm d}r. \quad (8)$$

Here $n, l$ are the quantum numbers of $N_2$ equivalent valence electrons, $\begin{bmatrix} j_2' & 2 & j_2 \\ m_2 & 0 & m_2 \end{bmatrix}$-Clebsch-Gordan coefficients, $\begin{Bmatrix} L_2 & j_2 & S_2 \\ j_2' & L_2' & 2 \end{Bmatrix}$-6$j$-symbols, $\alpha_{\rm A}$-atomic polarisability of atom A. The reduced matrix elements $\left\langle (nl)^{N_2} S_2 L_2 \middle\| U^2 \middle\| (nl)^{N_2} S_2 L_2' \right\rangle$ depend on $l$ and $N_2$ only, and are given in [29] for $l = 1, 2$ and all possible values of $N_2$. The $\left\langle r_{\rm B}^2 \right\rangle_{nl}$ values were calculated in [30,31] from the Hartree-Fock orbitals for a large number of atoms and different $n$ and $l$.

The estimates of the dispersion interaction using the known atomic constants of rubidium showed that it is the largest within the DS configuration, though it does not exceed 44 cm$^{-1}$ for $R \approx 30$ a.u. For the SS and PP configurations it is even smaller and can be disregarded. It is important, however, that at distances larger than 36 a.u. the calculated molecular terms can be well approximated by the $-C/R^6$ dependence. For instance, at $R \approx 38$ a.u. the deviations of the $0_w^\sigma$ terms correlating with the $5{\rm D}_{3/2,5/2} + 5{\rm S}_{1/2}$ states from the $-C/R^6$ dependence do not exceed 4 cm$^{-1}$ in the worst case.

### 2.3 Non-diagonal interactions

Among the non-diagonal interactions the strongest is the dipole-dipole interaction that couples the initial SS and final DS configurations to the PP configuration. Note that the initial and final configurations are not directly coupled with each other since S↔S transitions are forbidden in any approximation. The coupling between the initial and final states of the system is put into effect thanks to their dipole interaction with the intermediate PP configuration. Matrix elements of the operator of dipole-dipole interaction,

$$\hat{V}_{\rm ABdip} = -\frac{2}{R^3} \sum_{q=-1}^{1} \frac{1}{(1-q)!(1+q)!} Q_{q{\rm A}}^{(1)} Q_{-q{\rm B}}^{(1)}, \qquad (9)$$

are easily calculable in the $|\Omega_w^\sigma\rangle$ basis by the methods of the theory of atomic spectra applying the Wigner-Eckart theorem [26]:

*see equation (10) below*

where [3×3] matrix is a 9$j$ symbol, but the reduced matrix elements $\langle \gamma j \| Q^{(1)} \| \gamma' j' \rangle$ of the irreducible tensor operators $Q_q^{(1)}$ are related to the experimentally measurable oscillator strengths of dipole transitions $f(\gamma j, \gamma' j')$ by the relation

$$f(\gamma j, \gamma' j') = \frac{2}{3} \frac{\varepsilon_{\gamma' j'} - \varepsilon_{\gamma j}}{2j+1} |\langle \gamma j \| Q^{(1)} \| \gamma' j' \rangle|^2. \qquad (11)$$

In equations (10, 11) $\gamma$ stays for all the quantum numbers characterising an atomic state, except the atomic spin $S$, the orbital moment $L$, and the total moment $j$, and $\varepsilon_{\gamma j}$ denotes the energy of a fine structure level.

Absolute values of the reduced matrix elements $\langle \gamma j \| Q^{(1)} \| \gamma' j' \rangle$ can be obtained from equation (11) by inserting the known values of oscillator strengths for rubidium. Note that equation (11) does not allow one to determine the sign of a matrix element. The sign can be determined from the comparison of the oscillator strengths calculated by the quantum defect method [32] with those measured experimentally. We assume that the method ensures the correct sign for a matrix element if the calculated oscillator strength agrees with the experimental value.

The rest of the non-diagonal matrix elements are negligible at large internuclear distances, since they decrease with the internuclear distance more rapidly than $R^{-3}$.

### 2.4 Molecular terms

Using the matrix elements calculated in the above described way, we obtain the molecular $\Omega_w^\sigma$ terms by diagonalising a number of $\hat{H}(\Omega_w^\sigma)$ matrixes,

$$\hat{H}(\Omega_w^\sigma) = \begin{pmatrix} \hat{E}_{\rm SS} + \hat{\alpha} Y_\Sigma({\rm SS}) & 0 & \hat{V}_{\rm dip}({\rm SS-PP}) \\ 0 & \hat{E}_{\rm SD} + \hat{\beta} Y_\Sigma({\rm DS}) & \hat{V}_{\rm dip}({\rm DS-PP}) \\ \hat{V}_{\rm dip}({\rm SS-PP}) & \hat{V}_{\rm dip}({\rm DS-PP}) & \hat{E}_{\rm PP} \end{pmatrix}, \qquad (12)$$

where $\hat{E}_{\rm SS}$, $\hat{E}_{\rm SD}$, $\hat{E}_{\rm PP}$ are diagonal matrixes, eigenvalues of which correspond to sums of energies of isolated atoms in the $7{\rm S}_{1/2}$+$5{\rm S}_{1/2}$, $5{\rm D}_{5/2,3/2}$+$5{\rm S}_{1/2}$, $5{\rm P}_{3/2,1/2}$+$5{\rm P}_{3/2,1/2}$ states, matrixes $\hat{\alpha}$ and $\hat{\beta}$ are built up from Clebsch-Gordan coefficients, but $\hat{V}_{\rm dip}({\rm SS-PP})$ and $\hat{V}_{\rm dip}({\rm DS-PP})$ are matrixes of dipole-dipole interaction between the SS and PP, and DS and PP configurations, respectively. The possible molecular terms that can arise from the $7{\rm S}_{1/2}$+$5{\rm S}_{1/2}$, $5{\rm D}_{5/2,3/2}$ + $5{\rm S}_{1/2}$, and $5{\rm P}_{3/2,1/2}$ + $5{\rm P}_{3/2,1/2}$ states are listed in Table 2. The numerical diagonalisation procedure of $\hat{H}(\Omega_w^\sigma)$ matrixes for different internuclear distances yielded a set of $Rb_2$ adiabatic terms given in Figure 2.

$$\left\langle \gamma_1 j_1 \gamma_2 j_2 j \Omega \middle| V_{\rm ABdip} \middle| \gamma_1' j_1' \gamma_2' j_2' j' \Omega' \right\rangle = \delta_{\Omega\Omega'} \left( -\frac{2}{R^3} \right) \left\langle \gamma_1 j_1 \middle\| Q_{\rm A}^{(1)} \middle\| \gamma_1' j_1' \right\rangle \left\langle \gamma_2 j_2 \middle\| Q_{\rm B}^{(1)} \middle\| \gamma_2' j_2' \right\rangle$$
$$\times \sum_{\chi q} \left[ (1-q)!(1+q)! \right]^{-1} \begin{bmatrix} 1 & 1 & \chi \\ q & -q & 0 \end{bmatrix} \begin{bmatrix} j' & \chi & j \\ \Omega' & 0 & \Omega \end{bmatrix} \left[ (2j'+1)(2\chi+1) \right]^{1/2} \begin{Bmatrix} \chi & j & j' \\ 1 & j_1 & j_1' \\ 1 & j_2' & j_2' \end{Bmatrix}, \qquad (10)$$

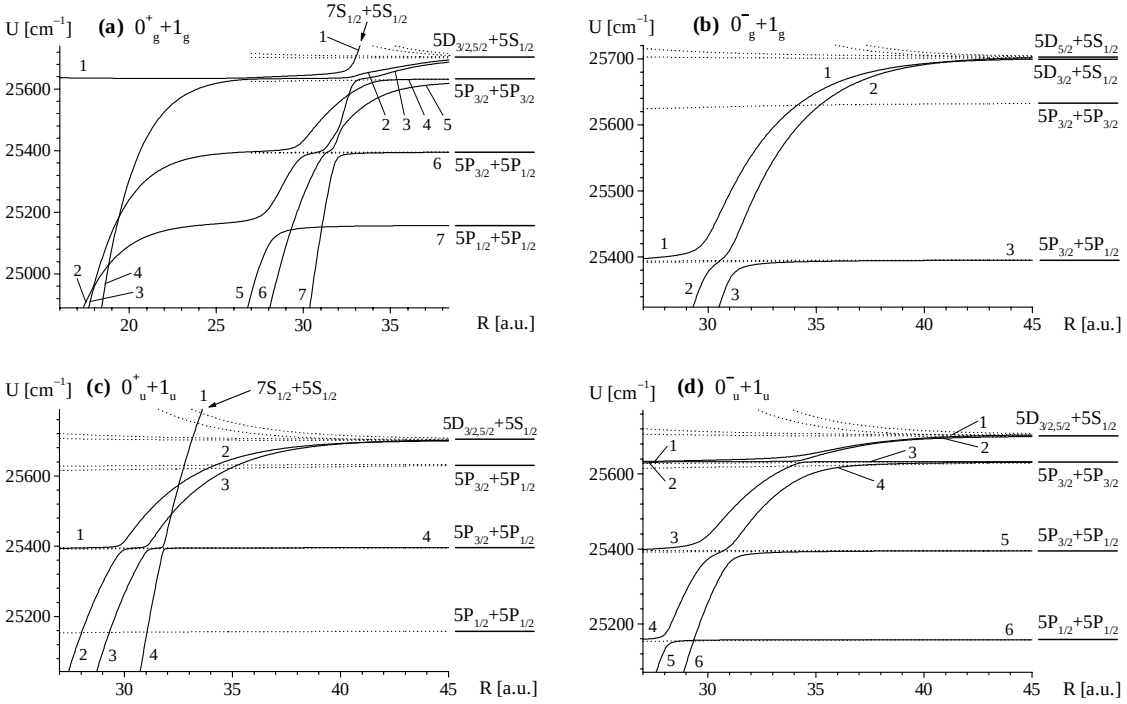


**Fig. 2.** Adiabatic molecular $\Omega^{\sigma}_{w}$ terms of $Rb_2$. The zero energy is chosen at the Rb(5S)+Rb(5S) dissociation limit of $Rb_2$. The number labels of terms correspond to the numbers of rows and columns in Tables 4–7. (a) $0^+_g$ (solid lines) and $1_g$ (dotted lines) terms; (b) $0^-_g$ (solid lines) and $1_g$ (dotted lines) terms; (c) $0^+_u$ (solid lines) and $1_u$ (dotted lines) terms; (d) $0^-_u$ (solid lines) and $1_u$ (dotted lines) terms.

**Table 2.** The number of molecular states with projections $\Omega = 0$, 1, 2 and 3 arising from the $S_{1/2}$+ $S_{1/2}$, $D_{5/2}$+ $S_{1/2}$, $D_{3/2}$+ $S_{1/2}$, $P_{3/2}$+ $P_{3/2}$, $P_{3/2}$+ $P_{1/2}$ and $P_{1/2}$+$P_{1/2}$ states of separated atoms.

| Molecular state | Atomic asymptote | | | | | |
|---|---|---|---|---|---|---|
| | $S_{1/2}$+$S_{1/2}$ | $D_{5/2}$+$S_{1/2}$ | $D_{3/2}$+$S_{1/2}$ | $P_{3/2}$+$P_{3/2}$ | $P_{3/2}$+$P_{1/2}$ | $P_{1/2}$+$P_{1/2}$ |
| $0^+_g$ | 1 | 1 | 1 | 2 | 1 | 1 |
| $0^-_g$ | 0 | 1 | 1 | 0 | 1 | 0 |
| $0^+_u$ | 1 | 1 | 1 | 0 | 1 | 0 |
| $0^-_u$ | 0 | 1 | 1 | 2 | 1 | 1 |
| $1_g$ | 1 | 2 | 2 | 1 | 2 | 0 |
| $1_u$ | 1 | 2 | 2 | 2 | 2 | 1 |
| $2_g$ | 0 | 2 | 1 | 1 | 1 | 0 |
| $2_u$ | 0 | 2 | 1 | 1 | 1 | 0 |
| $3_g$ | 0 | 1 | 0 | 0 | 0 | 0 |
| $3_u$ | 0 | 1 | 0 | 1 | 0 | 0 |

### 2.5 Influence of the ionic $Rb^+$+$Rb^-$ configuration

A quasi-molecule composed of two Rb atoms has also the ionic $Rb^+$+$Rb^-(^1S)$ configuration. The energy $E_{\rm ion}$ of this configuration changes with the internuclear distance as

$$E_{\rm ion} = -\frac{\beta^2}{2} - \frac{1}{R} - \frac{\alpha(\mathrm{Rb}^+) + \alpha(\mathrm{Rb}^-)}{R^4} + I_{\rm Rb},$$

with $\beta^2/2$ being the energy of electron affinity for Rb, $\alpha(\mathrm{Rb}^+)$, $\alpha(\mathrm{Rb}^-)$ – dipole polarisabilities of $Rb^+$ and $Rb^-$, $I_{\rm Rb}$ – the first ionisation potential of Rb atom. The ionic configuration perturbs the SS and DS configurations at $R \approx 63.6$ a.u. and $R \approx 54.0$ a.u., respectively. Therefore care was taken to estimate the ionic-covalent interaction in order to determine the possible contribution of ET through the ionic state.

The ionic-covalent interaction has been considered in a number of studies using the single-electron approximation to describe the motion of an active electron in the system $(\mathrm{A}^+ + e + \mathrm{B})$. The non-diagonal interaction matrix elements of the ionic configuration with the SS and DS configurations are of the form [33]

$$\langle nl|\hat{H}|i\rangle = \left[\frac{1}{2}(2l+1)\beta\right]^{1/2} N_i N_{nl} R^{\frac{1}{\alpha_{nl}}-1} \mathrm{e}^{-\alpha_{nl}R}.$$

We used here asymptotic representations for both the atomic wave function (see Eq. (6)) and the wave function of the electron in the negative ion,

$$\varphi_i(R) = N_i R^{-1} \mathrm{e}^{-\beta R}.$$

The normalising coefficients $N_i$ for a number of negative ions are tabulated in [34].

Adiabatic molecular terms can be obtained from diagonalisation of the corresponding matrix in basis of the ionic $Rb^+Rb^-$ state and a covalent state belonging to either SS or DS configuration. Because of the large internuclear distances the splittings of terms are exponentially

small. According to our calculations, they do not exceed 4.2 $cm^{-1}$ for the avoided crossing of the ionic and SS, and 14.3 $cm^{-1}$ for the ionic and DS configurations.

For the more complicated case when two excited electrons bind into covalent state as in the case of the PP configuration, the above model is inapplicable. There exists, however, a reason why the doubly excited PP configuration hardly mixes with the ionic one. Physically it is related to the fact that the weakly bound electron of the negative ion can hardly influence the valence electron of the atom. If one neglects this influence, the wave functions of the ionic configuration are orthogonal to the wave functions of the PP configuration. The coupling between these two configurations can be estimated following [7]. The ionic and covalent states are coupled by the dipole-dipole interaction (allowed dipole transitions Rb(5P)→Rb(5S) and Rb(5P)→$Rb^+ + e$). Non-diagonal matrix elements are calculable in the same manner as for the covalent states. We estimated the density of the oscillator strength $df/dE$ for the transition from 5P to continuum, needed for the calculations, as it was proposed in [35]. The splitting of terms turned out to be by an order of magnitude smaller than for the interaction of the ionic and DS configuration, therefore one can assume that the ionic and PP configurations practically do not interact.

We have not considered so far the interaction of covalent configurations with the excited ionic configuration with the negative Rb ion in the quasi-stationary $^3$P state. Since we do not know the energy of this state, we were unable to localise the corresponding non-adiabatic regions, neither could we determine if they are present at all. There exists, however, a consideration why the transitions *via* the excited ionic state, with the electronic configuration of $Rb^-(^3P)$ $nS^A np^A$, is not expected to be efficient. The electron in the negative ion is weakly coupled with the valence electron of the atom. If one neglects this coupling and represents the wave function of the electron undergoing a transition in form of multiplication of one-electron functions, then the wave function of the ionic configuration $\langle nS^A|\langle np^A|$ and those of excited covalent configurations are practically orthogonal. Therefore transitions through the excited ionic state are expected to proceed at relatively low efficiencies.

## 3 Non-adiabatic transitions and dynamics of the ET

The molecular terms obtained from diagonalisation of the $\hat{H}(\Omega_w^\sigma)$ matrix (12) allow us to study the dynamics of ET processes among the 7S, 5D and 5P states, and to calculate the corresponding transition probabilities and cross-sections. The large number of crossings and avoided crossings of terms at internuclear distances around 30 a.u. (*cf.* Figs. 2a–2d) are responsible for the large cross-sections of ET and quenching at small (thermal) collision energies. Since the regions of strong interaction are well localised and there is a rather large number of them, one can develop a relatively simple model in which the non-adiabatic regions are successively treated with no account for interference effects.

In the system of adiabatic $\Omega_w^\sigma$ terms the only reason for transitions among them is the motion of nuclei. If one neglects the transfer of electronic momentum, which in our case is of no considerable importance, then the operator of non-adiabatic coupling in rotating molecule coordinates is expressed as a sum of radial and tangential components:

$$\mathrm{i}\left\langle \Omega_w^\sigma \left| \frac{\partial}{\partial t} \right| \Omega_{w'}^{\prime\sigma'} \right\rangle = v_\mathrm{R} \left\langle \Omega_w^\sigma \left| \mathrm{i}\frac{\partial}{\partial R} \right| \Omega_{w'}^{\prime\sigma'} \right\rangle + \omega \langle \Omega_w^\sigma | \hat{j}_\perp | \Omega_{w'}^{\prime\sigma'} \rangle, \quad (13)$$

where $v_\mathrm{R}$ is the radial relative velocity of the colliding atoms, and $\omega$ is the angular velocity of the rotation of internuclear axis. At large internuclear distances, which correspond to Hund's case (c) coupling, the selection rules for the operator (13) are

$$\Delta\Omega = \pm 1 \ , \ g \leftrightarrow g \ , \ u \leftrightarrow u$$

for perturbations due to the rotation of internuclear axis (Coriolis interaction $V_\mathrm{Cor}$), and

$$\Delta\Omega = 0 \ , \ g \leftrightarrow g \ , \ u \leftrightarrow u, \ 0^+ \leftrightarrow 0^+ \ , \ 0^- \leftrightarrow 0^-$$

for perturbations due to the radial motion. These rules allow us to consider the systems of even and odd terms independently.

### 3.1 Perturbations due to the Coriolis interaction

The rotation of the internuclear axis causes transitions between terms of different symmetries, *i.e.*, between terms with $\Omega = 0$ and $\Omega = 1$. In the case of thermal collisions at large internuclear distances the Coriolis interaction is weak, therefore it is convenient to use perturbation theory.

In the system of $Rb_2$ terms, two types of rotational coupling are possible. The first type is the so called unlocalised coupling, which takes place when in a region of avoided crossing of two potential curves with equal $\Omega$ the mutual displacement of terms is such that along one or both asymptotes of the crossing curves there lie almost unperturbed terms with $\Omega' = \Omega \pm 1$. This is the case, for instance, in the system of $0_g^+ - 1_g$ terms (see Fig. 2a), where the unperturbed $1_g$ term correlating with the $5D_{5/2}$+$5S_{1/2}$ state lies along the asymptotes of the two avoided crossing $0_g^+$ terms correlating with $7S_{1/2}$+$5S_{1/2}$. Similar situations can be found also for some other terms correlating with other atomic states. Transition probability in this case can be calculated using the adiabatic perturbation theory:

$$P_{if} = \left| \int_{-\infty}^{+\infty} (\hat{V}_\mathrm{Cor})_{if} \exp\left\{ \mathrm{i} \int_t \Delta U_{if}(t')\mathrm{d}t' \right\} \mathrm{d}t \right|^2, \quad (14)$$

where $(\hat{V}_\mathrm{Cor})_{if}$ is the matrix element of Coriolis interaction between states $i$ and $f$, and $\Delta U_{if}$ is the energy difference of these two states. The matrix elements of Coriolis

interaction in $\Omega_w^\sigma$ basis are of the form [26]:

$$\langle \Omega_w^\sigma | \hat{V}_{\rm Cor} | \Omega_w'^\sigma \rangle = \frac{\lambda_+(J)\delta_{\Omega+1,\Omega'}\langle \Omega_w^\sigma | \hat{j}_\perp | \Omega_w'^\sigma \rangle + \lambda_-(J)\delta_{\Omega-1,\Omega'}\langle \Omega_w^\sigma | \hat{j}_\perp | \Omega_w'^\sigma \rangle}{\mu R^2}.$$

Here, $\mu$ is the reduced mass, and

$$\lambda_\pm(J) = \sqrt{(J \mp \Omega)(J \pm \Omega + 1)},$$

with $J$ being the total angular momentum of the system.

Using the straight trajectory approximation for calculation of integrals (14) and limiting the impact parameters to $\rho > 20$ a.u., we found that unlocalised rotational coupling gives insignificant contribution to the ET. It should be noted, however, that in the adiabatic case the main contribution to the transition probability is due to transitions at small internuclear distances in the vicinity of the turning point, for which the potential curves are not available. Therefore the final conclusion about the contribution of this type of coupling cannot be drawn yet.

The second type of Coriolis interaction corresponds to localised coupling, when the terms of different symmetries cross. In the system of terms with different $\Omega$, the crossing points are localised in the region of $27 \le R \le 33$ a.u. The transition probability at a single pass through the region of non-adiabaticity [24],

$$P_{if} = \frac{2\pi\omega_{\rm c}^2 \left| \langle \Omega_w^\sigma | \hat{j}_\perp | \Omega_w'^\sigma \rangle \right|^2}{|\Delta F_{\rm c}| v_{\rm c}}, \qquad (15)$$

is expressed through the parameters of the crossing point at $R = R_{\rm c}$ – the angular velocity $\omega_{\rm c}$ at the crossing point, the difference of slopes of the crossing terms,

$$|\Delta F_{\rm c}| = \left| \frac{\partial U(\Omega_w^\sigma)}{\partial R} - \frac{\partial U(\Omega_w'^\sigma)}{\partial R} \right|_{R=R_{\rm c}}, \qquad (16a)$$

and the radial velocity,

$$v_{\rm c} = v_\infty \sqrt{1 - \frac{\rho^2}{R_{\rm c}^2} - \frac{U_{\Omega_w^\sigma}(R_{\rm c}) - U_{\Omega_w^\sigma}(\infty)}{E_i}}, \qquad (16b)$$

where $v_\infty$ is the initial relative velocity of colliding atoms; $E_i$ and $U_{\Omega_w^\sigma}(\infty)$ are the kinetic and potential energies in the initial state, $U_{\Omega_w^\sigma}(R_{\rm c})$ is the potential energy of both terms at the crossing point. The parameters in (15, 16) are of simple physical meaning, and can be unambiguously determined for the case of crossing adiabatic terms.

In the region of crossing of two terms with different $\Omega$ it is a valid estimate

$$\langle \Omega_w^\sigma | \hat{j}_\perp | \Omega_w'^\sigma \rangle \sim 1.$$

It allows us to determine the maximum possible transition probability between the terms of different symmetry. The calculations show that for none of the crossing points does the transition probability exceed $10^{-2}$ upon twice passing the non-adiabatic region. It leads to ET cross-sections of an order of $10^{-16}$ cm$^2$, *i.e.*, about two orders of magnitude smaller than those observed in the experiment. Hence, the Coriolis interaction at large internuclear distances contributes insignificantly to the cross-sections of ET from 7S to 5D and collisional quenching of the 5D state.

### 3.2 Perturbations due to the radial motion

Perturbations due to the radial part of the operator of non-adiabatic interaction (13) induce transitions within the system of terms of the same symmetry. These transitions are localised within the non-adiabatic regions around the avoided crossings. As one can see from the potential curve diagrams (Figs. 2a–2d), the selection rule $\Delta\Omega = 0$ implies that only the terms with $\Omega = 0$ participate in this type of non-adiabatic interaction at large $R$. The exchange interaction brings together terms correlating with different atomic states, the strong dipole interaction of the PP configuration with the SS and DS configurations binds up the molecular states in a single block, but the radial motion of the nuclei gives rise to the non-adiabatic transitions among the terms. Initially the system of colliding atoms develops along one of the terms correlating with the initial state. Due to the rather large number of avoided crossings, after the collision the atoms will find themselves with a certain probability on any of the terms correlating with the final states. As it will be demonstrated below, this is the main mechanism of the ET in the system of the SS, DS, and PP configurations.

We begin the treatment of an ET process from a certain chosen state of separated atoms, and follow the redistribution of population probabilities of molecular states at successive passing of each of the avoided crossings as the nuclei approach each other. Since we do not know the terms at small internuclear distances, we consider reflection of probability flows from a hypothetical potential wall, and follow the development of the system in an outward direction towards the final states. The partial transition probabilities from a certain initial to a certain final molecular state are then used to calculate the effective ET cross-sections. The transition probability between two molecular states $m$ and $n$ are given by the well-known Landau-Zener formula:

$$P_{mn}(R_k, E_i, \rho) = \exp\left( - \frac{2\pi\varepsilon_k^2}{v_{R_k}|\Delta F_k|} \right), \qquad (17)$$

where $R_k$ is the coordinate of the centre of the $k$th avoided crossing of the two adiabatic terms, $\varepsilon_k = |\Delta U(R_k)|$ – the interaction matrix element between the two states, $|\Delta F_k|$ – the difference of slopes of diabatic terms:

$$|\Delta F_k| = \left| \frac{\partial U_m}{\partial R} - \frac{\partial U_n}{\partial R} \right|_{R=R_k}. \qquad (18)$$

The radial velocity $v_k$ at $R = R_k$ can be determined according to (16b), replacing the crossing point $R_{\rm c}$ with the crossing point of diabatic terms $R_k$ and taking the common energy of diabatic terms at their crossing point instead of $U_{\Omega_w^\sigma}(R_{\rm c})$.

**Table 3.** Landau-Zener parameters of avoided crossing between terms $m$ and $n$ with $\Omega = 0$. The term numbers correspond to the labels in Figures 2a–2d. The values in the last column give the influence of the avoided crossings $m/n$ on the cross-section.

| Avoided crossing $m$ / $n$ | $R_k$, a.u. | $U_k$, cm$^{-1}$ | $\varepsilon_k$, cm$^{-1}$ | $\lvert\Delta F_k\rvert$, cm$^{-1}$/a.u. | Influence of crossing $m$ / $n$ on the cross section*), % |
|---|---|---|---|---|---|
| $0_g^+$ terms (Fig. 2a) | | | | | $\sigma_{orig} = 2.32\times10^{-14}$ cm$^2$ |
| 2 / 3 | 17.98 | 24962.33 | 4.820 | 101.94 | 0 |
| 3 / 4 | 18.82 | 25030.44 | 0.430 | 238.83 | 0 |
| 2 / 3 | 19.40 | 25183.42 | 0.050 | 122.75 | 0.43 |
| 1 / 2 | 27.02 | 25634.48 | 2.388 | 2.33 | 0 |
| 4 / 5 | 28.12 | 25162.33 | 58.654 | 130.22 | 8.53 |
| 5 / 6 | 29.27 | 25141.56 | 1.297 | 160.48 | 0.86 |
| 3 / 4 | 29.80 | 25397.89 | 24.214 | 75.50 | 15.97 |
| 6 / 7 | 31.08 | 25155.19 | 3.004 | 332.55 | 2.80 |
| 4 / 5 | 31.21 | 25396.80 | 8.275 | 64.58 | 7.43 |
| 5 / 6 | 31.83 | 25391.03 | 29.328 | 177.01 | 51.34 |
| 4 / 5 | 32.05 | 25465.44 | 11.224 | 95.46 | 20.81 |
| 3 / 4 | 32.62 | 25583.26 | 1.542 | 131.77 | 2.80 |
| 2 / 3 | 33.19 | 25638.65 | 7.734 | 17.82 | 39.06 |
| 3 / 4 | 34.16 | 25632.39 | 8.325 | 12.35 | 7.33 |
| $0_g^-$ terms (Fig. 2b) | | | | | $\sigma_{orig} = 2.82\times10^{-14}$ cm$^2$ |
| 1 / 2 | 29.95 | 25401.62 | 26.900 | 68.02 | 58.67 |
| 2 / 3 | 31.04 | 25390.53 | 22.005 | 72.65 | 66.58 |
| 1 / 2 | 40.98 | 25695.31 | 0.350 | 0.47 | 65.63 |
| $0_u^+$ terms (Fig. 2c) | | | | | $\sigma_{orig} = 3.94\times10^{-14}$ cm$^2$ |
| 1 / 2 | 29.89 | 25396.49 | 10.570 | 85.64 | 70.71 |
| 2 / 3 | 31.07 | 25394.26 | 7.480 | 90.93 | 50.20 |
| 3 / 4 | 31.81 | 25394.35 | 7.310 | 260.11 | 50.02 |
| 2 / 3 | 32.16 | 25489.75 | 0.700 | 181.86 | 0 |
| 1 / 2 | 32.52 | 25574.37 | 0.380 | 188.55 | 41.50 |
| 2 / 3 | 40.88 | 25694.82 | 0.045 | 0.99 | 22.59 |
| $0_u^-$ terms (Fig. 2d) | | | | | $\sigma_{orig} = 0.47\times10^{-14}$ cm$^2$ |
| 4 / 5 | 28.09 | 25158.49 | 16.200 | 147.38 | 15.04 |
| 1 / 2 | 28.32 | 25633.47 | 1.125 | 2.51 | 0 |
| 5 / 6 | 29.34 | 25155.63 | 0.416 | 169.01 | 12.77 |
| 3 / 4 | 29.95 | 25401.79 | 31.685 | 61.67 | 70.71 |
| 4 / 5 | 31.07 | 25388.76 | 21.225 | 74.98 | 72.23 |
| 2 / 3 | 34.31 | 25633.32 | 3.195 | 18.84 | 50.26 |
| 1 / 2 | 38.64 | 25688.44 | 0.975 | 0.30 | 101.47 |

*) These quantities are calculated using expression $\frac{1}{2}\frac{\sqrt{(\sigma_1-\sigma_{orig})^2+(\sigma_2-\sigma_{orig})^2}}{\sigma_{orig}}\times100\%$, where $\sigma_{orig}$ is the original cross section with all parameters of avoided crossings accordingly included, $\sigma_1$ is the cross section at purely adiabatic passage through avoided crossing $m$ / $n$, and $\sigma_2$ is the cross section at purely diabatic passage through avoided crossing $m$ / $n$.

The parameters entering equations (17, 18) can be unambiguously determined only for the two-level case, when it is possible to rationally define the diabatic states. For the multichannel case the diabatic states cannot be well defined for all values of $R$, which leads to uncertainties in the values of the parameters. Therefore we applied a numerical procedure to determine the parameters directly from the term diagrams. We chose the coordinate $R_k$ of the centre of the non-adiabatic region equal to the internuclear distance at which the splitting between adiabatic molecular terms is minimal, and the interaction matrix element $\varepsilon_k$ equal to a half of this splitting. The values of $|\Delta F_k|$ were determined from the diabatic states obtained by a numerical procedure of diabatisation of the adiabatic states in the vicinity of avoided crossings. The values of the non-adiabatic parameters, as determined in the above way [36], are listed in Table 3. An alternative method to determine the Landau-Zener parameters from the adiabatic molecular terms proposed in [37] gives close values.

Most of the avoided crossings are well separated from each other. Hence, the application of the Landau-Zener model is fully justified. However, in two cases in the $0_g^+$ term system, and in one in $0_g^-$, the non-adiabatic regions are situated in an immediate proximity to each other, so that practically simultaneous coupling of three adiabatic states takes place. Although the use of the Landau-Zener model is not quite correct in such a case, the discrepancies that can arise in calculations of probabilities of independent transitions are practically compensated by integration over a large number of trajectories with different impact parameters and initial energies. The latter statement was verified by comparing the probabilities, obtained by successive application of Landau-Zener model, with the ones obtained from a numerical solution of a system of differential equations for the three-state-coupling case in the system of $0_g^-$ terms at $R \sim 30$ a.u.

To calculate the effective cross-sections, we used the procedure proposed in [19]. We assumed that initially (at $R = \infty$) only one molecular state is populated (with a unity probability), while all the other states are not. In the course of time, the system develops towards smaller $R$ and passes successively through all the non-adiabatic regions. At each of them redistribution of populations of molecular states takes place. Let the populations of adiabatic states $m$ and $n$ before passing the $k$th non-adiabatic region of the same symmetry $p$ be $W_m(t)$ and $W_n(t)$. Then, after passing the strong coupling region the respective populations for a given trajectory $(E_i, \rho)$ become

$$\tilde{W}_m = W_m[1 - P_{mn}(R_k, E_i, \rho)] + W_n P_{mn}(R_k, E_i, \rho), \tag{19a}$$

$$\tilde{W}_n = W_n[1 - P_{mn}(R_k, E_i, \rho)] + W_m P_{mn}(R_k, E_i, \rho), \tag{19b}$$

where $P_{mn}(R_k, E_i, \rho)$ is given by equation (17). The equation system (19) has to be solved successively for each avoided crossing that is passed in the course of collision, with the initial conditions $W_i(t_i) = 1$ and $W_n(t_i) = 0$ (here, $W_i(t_i)$ is the initial population of the initial molecular state, and $W_n(t_i)$ are the initial populations of all the other states).

At small internuclear distances we consider reflection of the population flows from a potential wall, after which the system develops in the outward direction. Let $W_n^{(i)}$ be the population of the $n$th state before the reflection. After the reflection this population becomes

$$W_n^{(r)} = W_n^{(i)}(1 - \kappa_n), \tag{20}$$

where $\kappa_n$ is the absorption coefficient on the wall for the state $n$. Since we do not know the behaviour of terms at small internuclear distances, we assumed that incident flows are completely reflected, *i.e.*, $\kappa_n = 0$, which ensures implementation of conservation of a total flow $\sum_n W_n = 1$ for all $R$. Variation of the value of $\kappa_n$ allows one to exclude

definite channels and to investigate their partial contributions to the ET. We used this variation also to investigate the possible contribution of processes at small $R$, *e.g.*, influence of the turning points. Although the non-adiabatic coupling in turning points can be strong, the localisation of these points at small $R$ leads to small contribution to the cross-section. Moreover, after the reflection the region of non-adiabatic coupling at large $R$ is passed again and it leads to redistribution which is weakly dependent on the population distribution after the reflection from the turning points. The calculations showed that a nearly final population distribution is established already after a single passage through the non-adiabatic region at large $R$. The above considerations allow us to assume that the region of small $R$ is not significantly contributing to the cross-section.

After the reflection, one has to consider development of the system in the outward direction, solving the equation system (19) for the reflected population flows, which provides the final populations of the molecular states $W_n^{(f)}(t_f)$. The partial effective cross-sections for decay of the system through channel $n$ are then obtained by integration over all the possible trajectories:

$$\sigma_n^p(i,E_i) = 2\pi\sqrt{\frac{E_{f,n}}{E_i}}\int_0^{\rho_{\max}} \rho W_n^{(f)}(i, t\to\infty)\mathrm{d}\rho, \quad (21)$$

where $i$ denotes the entrance channel, and $E_{f,n}$ is the final kinetic energy. The maximal impact parameter is limited by two conditions:

(a) during the collision the radial velocity $v_\mathrm{R} > 0$ at the crossing, *i.e.*, the radical in equation (16b) should always be real;

(b) for a given initial kinetic energy $E_i$ the system should classically overcome the centrifugal barrier in the entrance channel, *i.e.*,

$$E_i \geq U_{\mathrm{eff},i}(R_\mathrm{b}) = E(\mathrm{A}_i) + E(\mathrm{B}_i^*) + U_i(R_\mathrm{b}) + \frac{E_i\rho^2}{R_\mathrm{b}^2},$$

$$\left.\frac{\mathrm{d}U_{\mathrm{eff},i}}{\mathrm{d}R}\right|_{R=R_\mathrm{b}} = 0,$$

where $E(\mathrm{A}_i) + E(\mathrm{B}_i^*)$ is the total initial excitation energy at infinite internuclear separation, and $R_\mathrm{b}$ is the internuclear distance corresponding to the maximum point of the centrifugal barrier in the entrance channel.

We chose $\rho_{\max}$ as the smallest of the two limiting values, given by the conditions (a) and (b).

To obtain cross-sections comparable with the experimental ones, equation (21) should be averaged over the collision velocity distribution, which is Maxwellian in case of vapour cell experiments:

$$\sigma_n^p(i,T) = \int_{E_{\min}}^{\infty} \sigma_n^p(i,E_i)\exp\left(-\frac{E_i}{T}\right)\frac{1}{T^2}E_i\mathrm{d}E_i. \quad (22)$$

Here, $E_{\min}$ is the difference of electronic energies in the final and initial states, and it should be set equal to zero for exoenergetic processes. The effective cross-section for a certain ET process is then obtained by summing the partial cross-sections (22) over all initial states $i$ and symmetries $p$, and all states $n$ correlating with the chosen final atomic configuration:

$$\sigma(T) = \sum_i \sum_p \sum_n g_i^p \sigma_n^p(i,T),$$

where $g_i^p$ is the statistical weight of state $i$ of symmetry $p$, normalised so that $\sum_{i,p} g_i^p = 1$. Cross-sections $\sigma(T)$ are to be compared to the effective cross-sections determined from the experimentally measured rate constants.

## 4 ET cross-sections

The cross-sections $\sigma_n^p(i,E_i)$ were calculated in a broad range of temperatures from 400 to 1200 K for different symmetries of molecular states and all the possible scattering channels within each symmetry. The results are displayed in Tables 4–7. Each table gives partial effective cross-sections for different $\Omega_w^\sigma$ symmetries for transitions from an initial state to a number of final states. The cross-sections are given for two different temperatures, which makes possible approximations for intermediate temperature values. The total effective ET cross-sections are summarised in Table 8 for $T = 500$ K together with the available experimental data.

### 4.1 Rb(5D) + Rb(5S) collisions

We shall illustrate the use of data from Tables 4–7 on the example of quenching of the 5D state in collisions with ground state Rb atoms. The 5D state is split in two fine structure components with $j = 5/2$ and $3/2$. According to Table 2, 24 molecular states (including the doubly degenerate states with $\Omega \neq 0$) correlate with the $5\mathrm{D}_{5/2}$+$5\mathrm{S}_{1/2}$ states, and 16 – with $5\mathrm{S}_{1/2}$+$5\mathrm{D}_{3/2}$. If one assumes that the 5D state $j$-components are populated according to their statistical weights (which is reasonable under vapour cell conditions), then for $j = 5/2$ the probability that the colliding atoms will find themselves in the $0_g^+$ state is $(1/24)g_{j=5/2}$. Similarly, for collisions of ground state atoms with the atoms in the $5\mathrm{D}_{3/2}$ state this probability is $(1/16)g_{j=3/2}$. If the system develops in the $0_g^+$ state correlating with the $5\mathrm{D}_{5/2}$+$5\mathrm{S}_{1/2}$ initial configuration, the probabilities are the largest for transitions to the $0_g^+$ states correlating with the doubly excited $5\mathrm{P}_{3/2}$+$5\mathrm{P}_{3/2}$ and $5\mathrm{P}_{3/2}$+$5\mathrm{P}_{1/2}$ states of separated atoms. Transitions to the other states are considerably less efficient. In the case of the $0_g^+$ term correlating with the $5\mathrm{D}_{3/2}$+$5\mathrm{S}_{1/2}$ state the situation is analogous. The effective quenching cross-section of the 5D state through the $0_g^+$ terms can be then calculated by summing over all the sates $n$ and $k$ which

**Table 4.** Partial effective cross-sections ($cm^{-2}$) for the $0_g^+$ symmetry for transitions from an initial state to a final state. The numbering of rows and columns correspond to the labels of terms in Figure 2a.

| Initial state | $T$(K) | Final state | | | | |
|---|---|---|---|---|---|---|
| | | (1) $7S_{1/2}+5S_{1/2}$ | (2) $5D_{5/2}+5S_{1/2}$ | (3) $5D_{3/2}+5S_{1/2}$ | (4) $5P_{3/2}+5P_{3/2}$ | (5) $5P_{3/2}+5P_{3/2}$ |
| (1) $7S_{1/2}+5S_{1/2}$ | 500 | 7.85E-14 | 2.05E-14 | 2.21E-14 | 3.31E-14 | 1.11E-18 |
| | 700 | 6.86E-14 | 1.55E-14 | 1.69E-14 | 2.67E-14 | 8.06E-19 |
| (2) $5D_{5/2}+5S_{1/2}$ | 500 | 1.25E-15 | 1.86E-14 | 1.20E-14 | 1.17E-14 | 1.22E-14 |
| | 700 | 1.81E-15 | 1.92E-14 | 1.06E-14 | 1.12E-14 | 1.16E-14 |
| (3) $5D_{3/2}+5S_{1/2}$ | 500 | 1.35E-15 | 1.17E-14 | 1.66E-14 | 1.77E-14 | 1.03E-14 |
| | 700 | 1.99E-15 | 1.04E-14 | 1.51E-14 | 1.54E-14 | 8.06E-15 |
| (4) $5P_{3/2}+5P_{3/2}$ | 500 | 1.66E-15 | 8.05E-15 | 1.19E-14 | 1.99E-14 | 5.82E-15 |
| | 700 | 2.78E-15 | 8.48E-15 | 1.14E-14 | 1.72E-14 | 4.94E-15 |
| (5) $5P_{3/2}+5P_{3/2}$ | 500 | 4.95E-20 | 8.37E-15 | 6.64E-15 | 5.81E-15 | 6.20E-14 |
| | 700 | 7.16E-20 | 8.83E-15 | 5.77E-15 | 4.93E-15 | 6.16E-14 |
| (6) $5P_{3/2}+5P_{1/2}$ | 500 | 1.32E-19 | 5.19E-15 | 5.05E-15 | 4.84E-15 | 5.43E-15 |
| | 700 | 2.52E-19 | 7.06E-15 | 6.16E-15 | 5.46E-15 | 6.17E-15 |
| (7) $5P_{1/2}+5P_{1/2}$ | 500 | 3.26E-20 | 2.15E-16 | 5.33E-16 | 4.97E-16 | 2.14E-16 |
| | 700 | 8.53E-20 | 3.58E-16 | 1.05E-15 | 8.09E-16 | 2.99E-16 |

**Table 5.** Partial effective cross-sections ($cm^{-2}$) for the $0_g^-$ symmetry for transitions from an initial state to a final state. The numbering of rows and columns correspond to the labels of terms in Figure 2b.

| Initial state | $T$(K) | Final state | | |
|---|---|---|---|---|
| | | (1) $5D_{5/2}+5S_{1/2}$ | (2) $5D_{3/2}+5S_{1/2}$ | (3) $5P_{3/2}+5P_{1/2}$ |
| (1) $5D_{5/2}+5S_{1/2}$ | 500 | 5.10E-14 | 2.75E-14 | 6.30E-14 |
| | 700 | 4.81E-14 | 2.45E-14 | 5.49E-14 |
| (2) $5D_{3/2}+5S_{1/2}$ | 500 | 2.70E-14 | 7.48E-14 | 2.82E-14 |
| | 700 | 2.41E-14 | 6.84E-14 | 2.67E-14 |
| (3) $5P_{3/2}+5P_{1/2}$ | 500 | 1.44E-14 | 6.77E-15 | 5.01E-14 |
| | 700 | 1.83E-14 | 9.40E-15 | 4.58E-14 |

**Table 6.** Partial effective cross-sections ($cm^{-2}$) for the $0_u^+$ symmetry for transitions from an initial state to a final state. The numbering of rows and columns correspond to the labels of terms in Figure 2c.

| Initial state | $T$(K) | Final state | | | |
|---|---|---|---|---|---|
| | | (1) $7S_{1/2}+5S_{1/2}$ | (2) $5D_{5/2}+5S_{1/2}$ | (3) $5D_{3/2}+5S_{1/2}$ | (4) $5P_{3/2}+5P_{1/2}$ |
| (1) $7S_{1/2}+5S_{1/2}$ | 500 | 1.55E-13 | 5.62E-16 | 9.38E-16 | 8.93E-15 |
| | 700 | 1.48E-13 | 4.93E-16 | 8.10E-16 | 7.59E-15 |
| (2) $5D_{5/2}+5S_{1/2}$ | 500 | 4.06E-17 | 1.08E-13 | 2.73E-15 | 2.18E-14 |
| | 700 | 6.89E-17 | 1.02E-13 | 2.32E-15 | 1.82E-14 |
| (3) $5D_{3/2}+5S_{1/2}$ | 500 | 6.66E-17 | 2.67E-15 | 8.51E-14 | 3.94E-14 |
| | 700 | 1.11E-16 | 2.28E-15 | 8.13E-14 | 3.32E-14 |
| (4) $5P_{3/2}+5P_{1/2}$ | 500 | 2.03E-16 | 4.85E-15 | 8.95E-15 | 4.26E-14 |
| | 700 | 4.44E-16 | 5.86E-15 | 1.09E-14 | 4.55E-14 |

do not correlate with the $5D_j+5S_{1/2}$ states:

$$\sigma^{0_g^+}(T) = g^{0_g^+}_{j=5/2} g_{j=5/2} \sum_n \sigma_n^{0_g^+}(T) + g^{0_g^+}_{j=3/2} g_{j=3/2} \sum_k \sigma_k^{0_g^+}(T).$$

Inserting here

$$g^{0_g^+}_{j=5/2} = 1/24, \;\; g_{j=5/2} = 3/5,$$
$$g^{0_g^+}_{j=3/2} = 1/16, \;\; g_{j=3/2} = 2/5,$$

and the corresponding $\sigma_n^{0_g^+}(T)$ values from Table 4, we obtain $\sigma^{0_g^+}$ (500 K) $= 2.6 \times 10^{-15}$ cm$^2$. In a similar way contributions due to transitions within systems of terms of other symmetries can be obtained from Tables 5–7.

The main contribution to the quenching of the 5D state is due to transitions induced by radial motion among the terms with zero projection of the total angular momentum onto internuclear axis. These transitions lead to the cross-section

$$\sigma_q^{5D}(500\text{ K}) \approx \sigma^{0_g^+} + \sigma^{0_u^+} + \sigma^{0_g^-} + \sigma^{0_u^-}$$
$$= 2.6 \times 10^{-15} + 1.6 \times 10^{-15} + 2.3 \times 10^{-15} + 1.5 \times 10^{-15}$$
$$= 8 \times 10^{-15}\text{ cm}^2,$$

which is close to the experimental value $\sigma_q^{5D,exp} = (2 \pm 1) \times 10^{-14}$ cm$^2$ [21]. The 5D state is quenched mainly

**Table 7.** Partial effective cross-sections ($cm^{-2}$) for the $0_u^-$ symmetry for transitions from an initial state to a final state. The numbering of rows and columns correspond to the labels of terms in Figure 2d.

| Initial state | $T$(K) | Final state | | | | |
|---|---|---|---|---|---|---|
| | | (1) $5D_{5/2}+5S_{1/2}$ | (2) $5D_{3/2}+5S_{1/2}$ | (3) $5P_{3/2}+5P_{3/2}$ | (4) $5P_{3/2}+5P_{3/2}$ | (5) $5P_{3/2}+5P_{1/2}$ |
| (1) $5D_{5/2}+5S_{1/2}$ | 500 | 3.69E-14 | 3.15E-14 | 1.45E-14 | 6.04E-15 | 8.36E-15 |
| | 700 | 3.62E-14 | 2.87E-14 | 1.19E-14 | 6.42E-15 | 9.73E-15 |
| (2) $5D_{3/2}+5S_{1/2}$ | 500 | 3.10E-14 | 4.35E-14 | 1.61E-14 | 3.85E-15 | 4.71E-15 |
| | 700 | 2.83E-14 | 4.29E-14 | 1.34E-14 | 3.27E-15 | 4.30E-15 |
| (3) $5P_{3/2}+5P_{3/2}$ | 500 | 9.35E-15 | 1.06E-14 | 4.97E-14 | 7.60E-16 | 8.99E-16 |
| | 700 | 8.56E-15 | 9.82E-15 | 5.17E-14 | 6.53E-16 | 8.24E-16 |
| (4) $5P_{3/2}+5P_{3/2}$ | 500 | 4.31E-15 | 2.55E-15 | 7.59E-16 | 4.32E-14 | 5.26E-14 |
| | 700 | 5.01E-15 | 2.41E-15 | 6.53E-16 | 4.19E-14 | 4.65E-14 |
| (5) $5P_{3/2}+5P_{1/2}$ | 500 | 2.31E-15 | 1.10E-15 | 2.78E-16 | 1.63E-14 | 4.66E-14 |
| | 700 | 3.8E-15 | 1.48E-15 | 3.49E-16 | 1.93E-14 | 4.22E-14 |
| (6) $5P_{1/2}+5P_{1/2}$ | 500 | 4.51E-16 | 2.32E-16 | 6.19E-17 | 3.79E-15 | 4.03E-15 |
| | 700 | 8.62E-16 | 3.62E-16 | 8.95E-17 | 5.08E-15 | 5.35E-15 |

in the reverse energy pooling processes

$$\mathrm{Rb(5D)} + \mathrm{Rb(5S)} \rightarrow \mathrm{Rb(5P_{3/2})} + \mathrm{Rb(5P_{3/2})}, \quad (23a)$$

$$\mathrm{Rb(5D)} + \mathrm{Rb(5S)} \rightarrow \mathrm{Rb(5P_{3/2})} + \mathrm{Rb(5P_{1/2})}, \quad (23b)$$

$$\mathrm{Rb(5D)} + \mathrm{Rb(5S)} \rightarrow \mathrm{Rb(5P_{1/2})} + \mathrm{Rb(5P_{1/2})}. \quad (23c)$$

The total effective cross-section for the process (23a) is $\sigma_{5\mathrm{D}\rightarrow 5\mathrm{P}_{3/2}+5\mathrm{P}_{3/2}} = 2.3 \times 10^{-15}$ cm$^2$, and it proceeds mainly through the $0_g^+$ and $0_u^-$ terms with approximately the same efficiency. For the process (23b) $\sigma_{5\mathrm{D}\rightarrow 5\mathrm{P}_{3/2}+5\mathrm{P}_{1/2}} = 5.2 \times 10^{-15}$ cm$^2$, a half of which is due to transitions within the $0_g^-$ term system, and the rest within the $0_g^+$ and $0_u^+$, $0_u^-$ terms. The process (23c) is relatively inefficient, with a cross-section $\sigma_{5\mathrm{D}\rightarrow 5\mathrm{P}_{1/2}+5\mathrm{P}_{1/2}} = 3.6 \times 10^{-16}$ cm$^2$.

**Table 8.** Theoretical and experimental cross-sections for collisional ET processes in rubidium vapour.

| Process | Cross sections (units of $10^{-15}$cm$^2$) | |
|---|---|---|
| | This work, theoretical (500 K) | Experimental, Ref. [21] |
| Rb($5D$)+Rb($5S$) → Rb($5P_{3/2}$)+Rb($5P_{3/2}$) | 2.3 | |
| Rb($5D$)+Rb($5S$) → Rb($5P_{3/2}$)+Rb($5P_{1/2}$) | 5.25 | |
| Rb($5D$)+Rb($5S$) → Rb($5P_{1/2}$)+Rb($5P_{1/2}$) | 0.36 | |
| Rb($7S$)+Rb($5S$) → Rb($5D$)+Rb($5S$) | 7.0 | 8±4 |
| Rb($7S$)+Rb($5S$) → Rb($5P_{3/2}$)+Rb($5P_{3/2}$) | 5.5 | |
| Rb($7S$)+Rb($5S$) → Rb($5P_{3/2}$)+Rb($5P_{1/2}$) | 1.5 | |
| Rb($7S$)+Rb($5S$) → Rb($5P_{1/2}$)+Rb($5P_{1/2}$) | 0.001 | |
| Rb($5D$)+Rb($5S$) quenching | ≤ 37 | 20±10 |

## 4.2 Rb(7S) + Rb(5S) collisions

In collisions of atoms in the 7S state with ground state atoms there can take place ET to the 5D state in the process (1). The total effective cross-section for this ET process, as obtained by summing contributions of all the possible channels, is $\sigma_{7\mathrm{S}\rightarrow 5\mathrm{D}}$ (500 K) $= 7 \times 10^{-15}$ cm$^2$, which is in a very good agreement with the value $(8 \pm 4) \times 10^{-15}$ cm$^2$ measured in the experiment [21].

Besides the process (1), also a reverse energy pooling is possible, which leads to population of the resonance states:

$$\mathrm{Rb(7S)} + \mathrm{Rb(5S)} \rightarrow \mathrm{Rb(5P_{3/2})} + \mathrm{Rb(5P_{3/2})}. \quad (24a)$$

$$\mathrm{Rb(7S)} + \mathrm{Rb(5S)} \rightarrow \mathrm{Rb(5P_{3/2})} + \mathrm{Rb(5P_{1/2})}. \quad (24b)$$

$$\mathrm{Rb(7S)} + \mathrm{Rb(5S)} \rightarrow \mathrm{Rb(5P_{1/2})} + \mathrm{Rb(5P_{1/2})}. \quad (24c)$$

The most efficient here is the population of resonance states with $j = j' = 3/2$ in transitions within the $0_g^+$ term system induced by the radial motion. The total cross-section for this process at $T = 500$ K is $\sigma_{7\mathrm{S}\rightarrow 5\mathrm{P}_{3/2}+5\mathrm{P}_{3/2}} = 5.5 \times 10^{-15}$ cm$^2$.

Transfer to the states with $j = 3/2$ and $j' = 1/2$ is also considerable. It proceeds at a cross-section $\sigma_{7\mathrm{S}\rightarrow 5\mathrm{P}_{3/2}+5\mathrm{P}_{1/2}}$ (500 K) $= 1.5 \times 10^{-15}$ cm$^2$. In this case the main contribution is due to the transitions within the $0_u^+$ term system. The dipole-dipole interaction couples the $0_u^+$ term of the 7S+5S configuration with the $0_u^+$ term correlating with $5\mathrm{P}_{3/2}+5\mathrm{P}_{1/2}$. In the same time, the $0_u^+$ term correlating with the 5D+5S states practically does not interact with the upper $0_u^+$ term.

Population of the states with $j = j' = 1/2$ in the process (24c) is considerably less efficient, and its cross-section does not exceed $\sigma_{7\mathrm{S}\rightarrow 5\mathrm{P}_{1/2}+5\mathrm{P}_{1/2}}$ (500 K) $= 1 \times 10^{-18}$ cm$^{-2}$. The total 7S state quenching cross-section due to processes (1) and (24a–24c) is $\sigma_q^{7\mathrm{S}}$ (500 K) $= 1.4 \times 10^{-14}$ cm$^2$.

### 4.3 5D state quenching through capture

The above described calculations are based on the assumption that the energy transfer is caused by essentially the non-adiabatic processes at large internuclear distances. We notice, however, that the experimental 5D quenching cross-section is about two times the calculated value (see Sect. 4.1). It indicates that there may exist inelastic processes at small internuclear distances, which lead to additional losses of population.

A possibility to estimate the maximum possible quenching cross-section through the capture cross-section is discussed in [38]. One can interpret the quenching cross-section as a sum of capture cross-sections on each of the attractive adiabatic terms correlating with the 5D+5S states. The capture cross-section is defined as

$$\sigma_{\rm capt} = \pi\rho_{\rm c}^2, \tag{25}$$

where the critical impact parameter $\rho_{\rm c}$ at which capture occurs can be determined from the equation system:

$$U(R) + E_i\frac{\rho_{\rm c}^2}{R^2} = E_i, \tag{26a}$$

$$\frac{{\rm d}U}{{\rm d}R} - 2E_i\frac{\rho_{\rm c}^2}{R^3} = 0. \tag{26b}$$

Knowing adiabatic molecular terms at large internuclear distances, one can apply numerical methods to calculate $\rho_{\rm c}$ from (26) as a function of $E_i$. The $E_i$ dependent capture cross-section (25) should then be averaged over the collision velocity distribution to obtain $\langle\sigma_{\rm capt}(T)\rangle$. The quenching cross-section can be expressed through the latter value as

$$\sigma_q^{\rm 5D,max} = \frac{g_a}{g_i}\frac{g_f}{g_a+g_f}\langle\sigma_{\rm capt}(T)\rangle, \tag{27}$$

where $g_a$ is the statistical weight of the attractive terms correlating with the 5D+5S states; $g_i$ – statistical weight of all the terms correlating with these states; $g_f$ – statistical weight of all the final molecular states to which transitions from the 5D state are possible. The first factor on the right hand side of equation (27) gives the probability to enter an attractive term from the 5D+5S state, but the second denotes the transition probability to all the final states.

Numerical calculations according to (26, 27) give for the maximum 5D quenching cross-section $\sigma_q^{\rm 5D,max} = 3.7\times 10^{-14}$ cm$^2$, which is almost two times larger than the experimental value $(2\pm1)\times10^{-14}$ cm$^2$ [21]. A close value is obtained when the molecular terms are approximated by the $U(R) = -C/R^6$ dependence (see Sect. 2.2). In this case,

$$\langle\sigma_{\rm capt}(T)\rangle = 5.4\left(\frac{C}{k_{\rm B}T}\right)^{1/3}.$$

Calculating the van der Waals constant according to formulae in Section 2.2 for polarisation interaction, we obtain $\sigma_q^{\rm 5D,max} = 2.8\times10^{-14}$ cm$^2$.

## 5 Discussion and conclusions

The results of the present work allow us to conclude that the main mechanism leading to specific ET processes occurring at excitation of the 7S and 5D states are the non-adiabatic transitions at internuclear distances around 30 a.u. within the systems of terms of the same symmetry, induced by the radial motion of colliding atoms. The rotation of internuclear axis gives insignificant contribution to the ET in the case of localised coupling. The reason is the slow rotation of the internuclear axis at large internuclear distances, *i.e.*, weak Coriolis interaction.

The contribution of the ionic $Rb^+ + Rb^-$ configuration to the considered ET processes is negligible. The avoided-crossings of ionic and covalent states are situated at too large internuclear distances to provide remarkable coupling among the states. The influence of the ionic state is rather obstructive – it slightly redistributes the initial population flows over a large number of molecular states, decreasing somewhat the efficiencies of the ET processes. This effect becomes important for slow collisions, *e.g.*, collisions of trapped atoms. The influence of the ionic state weakens with increasing temperature because of the decrease in non-adiabatic transition probabilities.

We should mention one more fact related to the calculations of terms. Since the terms were calculated using a limited basis set of atomic states, the choice of this set may significantly influence the layout of terms. In our case it was enough to use the basis of three atomic configurations – SS, DS, and PP. Inclusion of the closest FS configuration practically did not change the layout of terms at large internuclear distances, since the exchange interaction dominating within the FS configuration is not strong enough to draw together terms of the FS and DS configurations at $R > 25$ a.u. Moreover, the SS and FS configurations interact very weakly, so that the SS configuration remains almost unperturbed.

The SS configuration is very important when the Rb(5D) + Rb(5S) → Rb(5P) + Rb(5P) process or the inverse to it energy pooling is concerned. The $Rb_2$ terms calculated in [6] in a similar manner as here but not including the SS configuration change considerably as this configuration is included. It explains the large difference between the results of present work and those of [6]. For instance, a number of new avoided crossings appear in the $0_g^+$ term system, which are not present in the calculations of [6]. The PP configuration plays a decisive role in the considered excitation transfer processes. Since in a number of cases the initial and final configurations are not directly coupled with each other (as in the case of ET from the 7S to 5D state), disregard of their coupling with the intermediate PP configuration would lead to negligible efficiencies of the corresponding ET processes (ET due to the Coriolis interaction and through the intermediate ion pair state). However, the PP configuration does not directly participate in the ET process (1). It only introduces a strong dipole coupling between the terms correlating with the SS and DS configurations, thus opening efficient channels for population of the 5D state. The latter assertion follows directly from our calculations: excluding

successively different scattering channels (*i.e.*, setting the absorption coefficient in Eq. (20) $\kappa_n = 1$) we found that molecular states of the PP configuration practically do not contribute to the population of the 5D state. Note also, that in the system of $0_u^+$ terms there is only one term correlating with the PP configuration, therefore dipole coupling between the SS and DS configurations is here by an order of magnitude weaker than in case of the $0_g^+$ terms, and the partial cross-section is correspondingly smaller. In the same time, transitions within the $0_u^+$ term system ensure efficient population of the $5P_{3/2}$+$5P_{1/2}$ states in process (23b).

The 5D and 7S states are efficiently quenched through the reverse energy pooling processes (23, 24), preferentially to the $5P_{3/2}$+$5P_{3/2}$ and $5P_{3/2}$+$5P_{1/2}$ doubly excited states. The most decisive here are the topology of molecular terms and the strengths of couplings among them rather than the energy defects of particular processes. It explains, for instance, why the cross-section for the process (23a), which has an energy defect of only 68 $cm^{-1}$, is more than two times smaller than the cross-section for the process (23b), the energy defect of which is as large as 306 $cm^{-1}$. It should be noted, however, that there exists an optimum coupling strength that gives the maximum transition probability. Too strong couplings lead to too large splitting of terms, and as a result the system develops adiabatically.

The dynamics of the 5D quenching is characterised by an almost homogeneous distribution of partial processes over the different $0_w^\sigma$ term systems (see Sect. 4.1). The contributions to the effective cross-section are approximately the same for terms of all $0_w^\sigma$ symmetries. Such a statistical nature of quenching processes justifies approximation of quenching by the averaged capture cross-section.

We should remark that in our case the cross-sections depend more strongly on the internuclear distance at which the non-adiabatic regions are located than on other parameters of the avoided crossings. The more avoided crossings are present in the system of terms of a given symmetry, the less pronounced is the significance of each particular crossing on the cross-section and the closer is the nature of the process to statistical. This is illustrated in the last column of Table 3, on the example of process $5D_{3/2} + 5S_{1/2} \rightarrow 5P_{3/2} + 5P_{1/2}$.

We find a very good agreement between our calculations and the experimental results of [21] for the process (1) (see Tab. 8). This experimental value is rather reliable, since it is determined from the measurements of relative fluorescence intensities not affected by the radiation trapping. The latter leads to large uncertainties in the determination of absolute concentrations of excited atoms and thus constitutes a serious problem in experimental studies involving resonance atoms as either collision partners or end products. For the reverse energy pooling (processes (23, 24)) cross-sections no experimental counterparts exist. Recalculation of the cross-sections from the direct energy pooling data of [6,15] using the detailed balancing principle is inappropriate since we have to do with a multichannel case, when the initial and final channels interact with other near lying states. The probability of each population transfer depends thus on the particular sequences of non-adiabatic interactions, and detailed balancing under such conditions is not valid. We therefore consider the direct energy pooling separately and the results will be reported elsewhere.

In conclusion, we have calculated cross-sections for inelastic processes occurring at excitation of 7S and 5D states of Rb. The asymptotic approach used in this work gives a very good agreement with the experimental results for the ET process (1). The doubly excited 5P+5P configuration acts here as a sort of carrier of the dipole-dipole interaction, although this configuration itself does not directly participate in the process. The theoretical quenching cross-section for the 5D state turned out to be about two times smaller than the experimental one, indicating that there might be other inelastic processes at small internuclear distances adding to the collisional depletion of the 5D state. The upper limit of the quenching cross-section can be estimated in a simple way using the averaged capture cross-section, still exact quantum chemical term calculations are necessary to draw conclusions about possible contribution of the processes at small $R$.

This work was supported by the Latvian Science Council, Grant No. 889. A.E. thanks Prof. K. Bergmann for the hospitality during his visit to Kaiserslautern, where some of the work on this manuscript has been done.

## References

1. L. Krause, Adv. Chem. Phys. **28**, 267 (1975).
2. E.E. Nikitin, Adv. Chem. Phys. **28**, 317 (1975).
3. A.N. Klucharev, A.V. Lazarenko, Opt. Spektrosk. **34**, 425 (1973).
4. M. Allegrini, G. Alzetta, A. Kopystynska, L. Moi, G. Orriols, Opt. Commun. **19**, 96 (1976).
5. V.M. Borodin, I.V. Komarov, Opt. Spectrosc. **36**, 145 (1974) [Opt. Spektrosk. **36**, 250 (1974)].
6. L. Barbier, M. Chéret, J. Phys. B **16**, 3213 (1983).
7. P. Kowalczyk, J. Phys. B **17**, 817 (1984); Chem. Phys. Lett. **68**, 203 (1979).
8. Zh.L. Shvegzhda, S.M. Papernov, M.L. Janson. Chem. Phys. Lett. **101**, 187 (1983).
9. J. Huennekens, A. Gallagher, Phys. Rev. A **27**, 771 (1983); S.A. Davidson, J.F. Kelly, A. Gallagher, *ibid.* **33**, 3756 (1986).
10. M. Allegrini, P. Bicchi, L. Moi, Phys. Rev. A **28**, 1338 (1983); M. Allegrini, C. Gabbanini, L. Moi, R. Colle, *ibid.* **32**, 2068 (1985).
11. Z.J. Jabbour, R.K. Namiotka, J. Huennekens, M. Allegrini, S. Milošević, F. de Tomasi, Phys. Rev. A **54**, 1372 (1996); F. de Tomasi, S. Milošević, P. Verkerk, A. Fioretti, M. Allegrini, Z.J. Jabbour, J. Huennekens, J. Phys. B **30**, 4991 (1997).
12. C. Vadla, K. Niemax, J. Brust, Z. Phys. D **37**, 241 (1996); C. Vadla, Eur. Phys. J. D **1**, 259 (1998).

13. R. K. Namiotka, J. Huennekens, M. Allegrini, Phys. Rev. A **56**, 514 (1997).
14. S. Gozzini, S.A. Abdullah, M. Allegrini, A. Cremoncini, L. Moi, Opt. Commun. **63**, 97 (1987).
15. C. Gabbanini, S. Gozzini, G. Squadrito, M. Allegrini, L. Moi, Phys. Rev. A **39**, 6148 (1989).
16. S. Guldberg-Kjær, G. De Filippo, S. Milošević, S. Magnier, J.O.P. Pedersen, M. Allegrini, Phys. Rev. A **55**, R2515 (1997); G. De Filippo, S. Guldberg-Kjær, S, Milošević, J.O.P. Pedersen, M. Allegrini, *ibid.* **57**, 255 (1998).
17. J.H. Nijland, J.A. de Gouw, C.J.G.J. Uiterwaal, H.A. Dijkerman, H.G.M. Heideman, J. Phys. B **23**, L553 (1990); J.H. Nijland, J.A. de Gouw, H.A. Dijkerman, H.G.M. Heideman, *ibid.* **25**, 2841 (1992); J.H. Nijland, J.J. Blangé, H. Rudolph, H.A. Dijkerman, H.G.M. Heideman, *ibid.* **25**, 4835 (1992).
18. P.H.T. Philipsen, J.H. Nijland, H. Rudolph, H.G.M. Heideman, J. Phys. B **26**, 939 (1993).
19. I.Yu. Yurova, O. Dulieu, S. Magnier, F. Masnou-Seeuws, V.N. Ostrovskii, J. Phys. B **27**, 3659 (1994).
20. I.Yu. Yurova, J. Phys. B **28**, 999 (1995).
21. Luo Caiyan, A. Ekers, J. Klavins, M. Jansons, Phys. Scripta **53**, 306 (1996).
22. A. Ekers, J. Alnis, Latv. J. Phys. Techn. Sci. **1**, 64 (1999); A. Ekers, Proc. Latv. Acad. Sci. B **7/8**, 130 (1995).
23. V. Grushevsky, M. Jansons, K. Orlovsky, Phys. Scripta **56**, 245 (1997).
24. B.M. Smirnov, *Asimptoticheskie metody v teorii atomnyh stolknovenij* [Asymptotic methods in the theory of atomic collisions] (Atomizdat., Moscow, 1973).
25. E.E. Nikitin, B.M. Smirnov, *Medlennye atomnye stolknovenija* [Slow atomic collisions, in *Russian*] (Energoatomizdat, Moscow, 1990).
26. E.E. Nikitin, S.Ja. Umanskii, *Theory of Slow Atomic Collisions* (Springer, Berlin, 1984).
27. I.I. Sobelman, *Vvedenije v teoriju atomnyx spektrov* [Introduction to the theory of atomic spectra] (Nauka, Moscow, 1977).
28. S.Ja. Umanskii, E.E. Nikitin, Theor. Chim. Acta **13**, 91 (1969); S.Ja. Umanskii, A.I. Voronin, *ibid.* **12**, 166 (1968).
29. I.I. Sobelman, *Atomic Spectra and Radiative Transitions* (Springer Ser. Chem. Phys., Springer, Berlin, 1979), Vol. 1.
30. V.F. Bratsev, *Tablitsy Atomnykh Funktsii* [Tables of Atomic Functions, in *Russian*] (Nauka, Leningrad, 1966); *Tablitsy Atomnykh Volnovykh Funktsii* [Tables of Atomic Wave Functions, in *Russian*] (Nauka, Leningrad, 1971).
31. A.A. Radtsig, B.M. Smirnov, *Spravochnik po Atomnoi i Molekulyarnoi Fizike* [Handbook of Atomic and Molecular Physics, in *Russian*] (Atomizdat, Moscow, 1980).
32. V.A. Davydkin, B.A. Zon, Opt. Spektrosk. (USSR) **51**, 25 (1981).
33. S. Magnier, M. Aubert-Frécon, O. Bouty, F. Masnou-Seeuws, Ph. Millie, V.N. Ostrovsky, J. Phys. B **27**, 1723 (1994).
34. A.A. Radzig, B.M. Smirnov, *Parametry atomov i atomnyh ionov* [Parameters of Atoms and Atomic Ions, in *Russian*] (Energoatomizdat, Moscow, 1986).
35. A. Burgess, M.J. Seaton, Mon. Not. R. Astron. Soc. **120**, 121 (1960).
36. The code used to calculate the non-adiabatic parameters is available upon request by K. Orlovsky.
37. H. Rudolf, M.F.V. Lundsgaard, in *Lasers, Atoms and Molecules: Dynamical Interactions*, Vulcano, Italy (HCM Network-Workshop, 1996), pp. 283-293.
38. E.I. Dashevskaya, A.I. Voronin, E.E. Nikitin, Can. J. Phys. **47**, 1237 (1969).
39. E.E. Nikitin, B.M. Smirnov, *Atomno-molekuljarnye processy v zadachah s reshenijami* [Atomic-Molecular Processes in tasks with solutions, in *Russian*] (Nauka, Moscow, 1988), p. 283.